

# MHD Flow Along a Vertical Plate with Heat and Mass Transfer under Ramped Plate Temperature

Mohammad Shareef

Department of Mathematics & Statistics, Integral University, Lucknow-226026, India

Received 25 Jan 2023

Accepted 30 Mar 2023

## Abstract

Present study is carried out to examine the effects of Porosity, thermophoresis, and rotation on the unsteady natural convective flow of an incompressible, viscous and electrically conducting fluid past an impulsively started vertical plate in a porous medium under the influence of a magnetic field with ramped wall temperature condition. Analytical solution of partial differential equations of the model is obtained by the Laplace transform method with the help of the Heaviside step function; also the expression for the Sherwood Number, Nusselt Number and Shear stress at the plate is obtained. The obtained results are checked against previously published work for special cases of the problem and found to be in excellent agreement. The results obtained are shown by graphs. The effect of physical parameters such as  $M$  (Magnetic parameter),  $K$  (Darcy permeability),  $Sr$  (Soret number) and  $\Omega$  (rotation parameter) on these fields are discussed in detail, and it has been observed that for both isothermal and ramped temperature plates; primary and secondary fluid velocity attain a different maximum value in the vicinity of the plate and then decrease gradually. The conclusions of the study have great applications in the field of science and engineering such as in rotating MHD induction machine energy generators, Magnetic field control of materials processing systems, planetary and solar plasma fluid dynamics systems, etc.

© 2023 Jordan Journal of Mechanical and Industrial Engineering. All rights reserved

**Keywords:** Ramped, Soret effect, Rotation, MHD, Porousmedium.

## Nomenclature

$D$	Mass diffusion coefficient
$G_m$	Mass Grashof number
$G_r$	Thermal Grashof number
$\alpha$	Thermal diffusivity
$K$	Permeability parameter
$S_c$	Schmidt number
$t'$	Dimensionless time
$k_T$	Thermal diffusion ratio
$u_0$	Constant speed of plate
$u$	Primary velocity of the fluid
$v'$	Dimensionless secondary velocity of the fluid
$\beta^*$	Volumetric coefficient of concentration expansion
$\nu$	Kinematic viscosity
$\mu$	Dynamic viscosity
$u'$	Dimensionless primary velocity of the fluid
$v$	Secondary velocity of the fluid
$g$	Acceleration due to gravity

$M$	Magnetic field parameter
$P_r$	Prandtl number
$S_r$	Soret number
$\rho$	Density of fluid
$D_T$	Thermal diffusion coefficient
$K'$	Dimensionless permeability parameter
$z'$	Dimensionless spatial coordinate normal to the plate
$\beta$	Volumetric coefficient of thermal expansion
$\theta$	Dimensionless temperature
$\phi$	Dimensionless concentration
$\Omega'$	Dimensionless rotation parameter

## 1. Introduction

In view of plentiful application in the field of science and engineering, such as nuclear reactors, MHD generators, space vehicle propulsion, induction pumps and oil exploration, some Significant researches have been done in the area of MHD flow. The magnetic field can control the thermo-physical properties of flow of an electrically conducting fluid. (Jaimala *et al.* [1], T.V. Laxmi and B. Shankar [2], Muthucumaraswamy and Prema [3], Branover [4], S. Ravi Kumar [5], Osalusi and Sibanda [6], Jawarneh *et al.* [7], Cowling [8]). Also, flow through a porous medium have great engineering and geophysical applications, viz, in petroleum technology to understand the movement of natural gas, oil and water through the oil

\* Corresponding author e-mail: rajputshareeflu@gmail.com.

reservoirs; in chemical engineering for purification and filtration process; in agriculture engineering to analyze the underground water resources. By virtue of these plentiful applications, a number of researchers have studied MHD flow with heat and mass transfer through a porous medium; a few of them are Singh and Kumar [9], Bala *et al.* [10], Kim [11], Mohammad *et al.* [12].

Moreover, the rotating fluids have their abundant geophysical and astrophysical applications. Some natural phenomena, such as hurricanes tornadoes, ocean circulations currents, etc. imply rotating flows with heat and mass transfer. Several books and research articles on hydrodynamic characteristics of rotating flows have been published: (Owen and Rogers [13], Greenspan [14], Jawarneh *et al.* [15]).

The temperature gradient difference plays an important role and generates the concentration flux inside the fluid, and this phenomenon is called Soret effect (Platten [16]). A numerical solution of oscillatory chemically-reacting MHD natural convection double-diffusive boundary layers in a porous medium with Soret and Dufour effects was studied by Bhargava *et al.* [17]. Postelnicu [18] analyzed the Soret and Dufour effects on MHD flow with heat and mass transfer by natural convection from vertical surface in a porous medium. Postelnicu [19] extended his work and analysed the influence of chemical reaction on heat and mass transfer by free convection from vertical surface in porous media considering the Soret and Dufour effects. Some research papers related to Soret effect and free convection have been published by Beg *et al.* [20], Alam and Rahman [21], Ibrahim [22], Anil Kumar *et al.* [24] and Ziya Uddin and Manoj Kumar [27 & 28]. This paper deals with the Soret effect under the temperature gradient due to ramped wall temperature condition.

Influenced by the above-discussed literature and applications, I [23] have extended my work from variable temperature to ramped wall temperature and compared the effect of various flow parameters in case of isothermal and ramped wall temperature. The Laplace transform method is used to solve the governing partial differential equations of the model. The influence of various parameters involved in the problem on velocity, temperature and concentration are discussed graphically.

## 2. Mathematical Calculation

Let us consider a coordinate system such as an infinite plate is lying in  $z=0$  plane and a magnetic field  $\vec{B}$  is applied normal to the plate. Both the plate and fluid are in a state of rigid body rotation with uniform angular velocity  $\vec{\Omega} = (0, 0, \Omega)$  about  $z$ -axis. Initially, the plate is at rest having a uniform temperature  $T_\infty$  and concentration  $C_\infty$ . At time  $t > 0$ , the plate suddenly begins to move vertically upward in its own plane in positive  $x$  direction with a velocity  $u_0$  and concentration are lowered or raised to  $C_p$ .

The initial and boundary conditions are taken as

$$\left. \begin{aligned} t \leq 0: u(z, t) = 0, v(z, t) = 0, T(z, t) = T_\infty, C(z, t) = C_\infty; \\ t > 0: u(0, t) = u_0, v(0, t) = 0, C(0, t) = C_\infty, T(0, t) = \begin{cases} \bar{T}_p, & t < t_0 \\ T_p, & t \geq t_0 \end{cases} \\ \text{and } u(z, t) \rightarrow 0, v(z, t) \rightarrow 0, T(z, t) \rightarrow T_\infty, C(z, t) \rightarrow C_\infty \text{ as } z \rightarrow \infty; \end{aligned} \right\} \quad (5)$$

At the same time the plate temperature is changed to  $\bar{T}_p$  ( $0 < t < t_0$ ) and  $T_p$  ( $t \geq t_0$ ). The movement of the plate and the free convection causes the fluid motion. Geometry of the problem (Imran *et al.* [25]) is presented in Fig. 1.

The governing PDEs of the models are non-linear but general characteristics of the fluid motion within the boundary layer can be analysed by simplified problem with some assumptions.

1. The plate is of infinite extent so all the physical variables can be considered as a function of  $t$  and  $z$  only.
2. All the fluid properties are constants and the variation in density is neglected everywhere except in the buoyancy term.
3. The fluid has small value of magnetic Reynolds number; hence the induced magnetic field can be neglected.
4. The fluid far away from the plate is undisturbed.
5. The plate is electrically non-conducting.
6. No polarization or applied voltages exist.

The governing equations of a viscous, incompressible and electrically conducting fluid under the above made assumptions are (Seth *et al.* [26]):

$$\frac{\partial u}{\partial t} - 2\Omega v = \nu \frac{\partial^2 u}{\partial z^2} + g\beta(T - T_\infty) + g\beta^*(C - C_\infty) + \frac{\sigma B_o^2}{\rho} u - \frac{\nu}{K} u \quad (1)$$

$$\frac{\partial v}{\partial t} + 2\Omega u = \nu \frac{\partial^2 v}{\partial z^2} - \frac{\sigma B_o^2}{\rho} v - \frac{\nu}{K} v \quad (2)$$

$$\frac{\partial T}{\partial t} = \frac{k}{\rho c_p} \frac{\partial^2 T}{\partial z^2} \quad (3)$$

$$\frac{\partial C}{\partial t} = D \frac{\partial^2 C}{\partial z^2} + \frac{D_T k_T}{T_m} \frac{\partial^2 T}{\partial z^2} \quad (4)$$

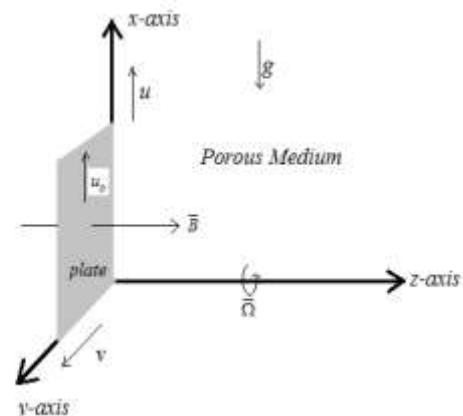


Figure 1. Geometry of the Problem

where  $\bar{T}_p = T_\infty + (T_p - T_\infty) \frac{t}{t_o}$  and  $t_o = \frac{\nu}{u_o^2}$ .

For converting the equation into dimensionless form, we use the following non-dimensional parameters and variables-

$$\left. \begin{aligned} u' &= \frac{u}{u_o}, v' = \frac{v}{u_o}, t' = \frac{u_o^2}{\nu} t, z' = \frac{u_o}{\nu} z, \theta = \frac{(T - T_\infty)}{(T_p - T_\infty)}, \phi = \frac{(C - C_\infty)}{(C_p - C_\infty)}, \\ P_r &= \frac{\nu}{\alpha}, M = \frac{\sigma B_o^2 \nu}{\rho u_o^2}, \Omega' = \frac{\nu}{u_o^2} \Omega, S_c = \frac{\nu}{D}, K' = \frac{u_o^2}{\nu^2} K, \\ G_m &= \frac{g \beta^* \nu (C_p - C_\infty)}{u_o^3}, S_r = \frac{D_T k_T (T_s - T_\infty)}{T_m \nu (C_s - C_\infty)}, G_r = \frac{g \beta \nu (T_p - T_\infty)}{u_o^3}. \end{aligned} \right\} \quad (6)$$

By using Eq. (6), Eqs. (1), (2), (3), (4) and (5) can be written as-

$$\frac{\partial u'}{\partial t'} - 2\Omega' v' = \frac{\partial^2 u'}{\partial z'^2} - (M + \frac{1}{K'})u' + G_r \theta + G_m \phi \quad (7)$$

$$\frac{\partial v'}{\partial t'} + 2\Omega' u' = \frac{\partial^2 v'}{\partial z'^2} - (M + \frac{1}{K'})v' \quad (8)$$

$$\frac{\partial \theta}{\partial t'} = \frac{1}{P_r} \frac{\partial^2 \theta}{\partial z'^2} \quad (9)$$

$$\frac{\partial \phi}{\partial t'} = \frac{1}{S_c} \frac{\partial^2 \phi}{\partial z'^2} + S_r \frac{\partial^2 \theta}{\partial z'^2} \quad (10)$$

$$\left. \begin{aligned} t' \leq 0 : u'(z', t') = 0, v'(z', t') = 0, \theta(z', t') = 0, \phi(z', t') = 0; \\ t' > 0 : u'(0, t') = 1, v'(0, t') = 0, \phi(0, t') = 1, \theta(0, t') = \begin{cases} t', & t' \leq 1 \\ 1, & t' > 1 \end{cases} \text{ and} \\ u'(z', t') \rightarrow 0, v'(z', t') \rightarrow 0, \theta(z', t') \rightarrow 0, \phi(z', t') \rightarrow 0 \text{ as } z' \rightarrow \infty. \end{aligned} \right\} \quad (11)$$

On combining Eqs. (7) and (8), we get,

$$\frac{\partial V'}{\partial t'} = \frac{\partial^2 V'}{\partial z'^2} - bV' + G_r \theta + G_m \phi \quad (12)$$

where  $V' = u' + iv'$  and  $i = \sqrt{-1}$ .

Also, the Eq. (11) changes as:

$$\left. \begin{aligned} t' \leq 0 : V'(z', t') = 0, \theta(z', t') = 0, \phi(z', t') = 0; \\ t' > 0 : V'(0, t') = 1, \phi(0, t') = 1, \theta(0, t') = \begin{cases} t', & t' \leq 1 \\ 1, & t' > 1 \end{cases} \text{ and} \\ V'(z', t') \rightarrow 0, \theta(z', t') \rightarrow 0, \phi(z', t') \rightarrow 0 \text{ as } z' \rightarrow \infty. \end{aligned} \right\} \quad (13)$$

For simplification we remove prime (') and above set of equations changes as

$$\frac{\partial V}{\partial t} = \frac{\partial^2 V}{\partial z^2} - bV + G_r \theta + G_m \phi \quad (14)$$

$$\frac{\partial \theta}{\partial t} = \frac{1}{P_r} \frac{\partial^2 \theta}{\partial z^2} \quad (15)$$

$$\frac{\partial \phi}{\partial t} = \frac{1}{S_c} \frac{\partial^2 \phi}{\partial z^2} + S_r \frac{\partial^2 \theta}{\partial z^2} \quad (16)$$

$$\left. \begin{aligned} t \leq 0 : V(z, t) = 0, \theta(z, t) = 0, \phi(z, t) = 0; \\ t > 0 : V(0, t) = 1, \phi(0, t) = 1, \theta(0, t) = \begin{cases} t, & t \leq 1 \\ 1, & t > 1 \end{cases} \text{ and} \\ V(z, t) \rightarrow 0, \theta(z, t) \rightarrow 0, \phi(z, t) \rightarrow 0 \text{ as } z \rightarrow \infty. \end{aligned} \right\} \quad (17)$$

Laplace transform method is used to solve the Eqs. (14), (15) and (16) with conditions prescribed in Eq. (17). Therefore, after applying the Laplace transform to the Eqs. (14), (15), (16) and using initial conditions, we get a set of equations in  $z$  and  $s$  as follows:

$$\frac{d^2}{dz^2} \bar{\theta}(z, s) - P_r s \bar{\theta}(z, s) = 0 \tag{18}$$

$$\frac{d^2}{dz^2} \bar{\phi}(z, s) - S_c s \bar{\phi}(z, s) = -S_c S_r \frac{\partial^2 \bar{\theta}(z, s)}{dz^2} \tag{19}$$

$$\frac{d^2}{dz^2} \bar{V}(z, s) - (b+s) \bar{V}(z, s) = -G_r \bar{\theta}(z, s) - G_m \bar{\phi}(z, s) \tag{20}$$

Under the changed boundary conditions

$$\bar{V}(0, s) = \frac{1}{s}, \quad \bar{V}(\infty, s) = 0 \tag{21}$$

where

$$\theta_1(z, t) = L^{-1} \left\{ \frac{e^{-z\sqrt{sP_r}}}{s^2} \right\} = -ze^{-\frac{z^2 P_r}{4t}} \frac{\sqrt{tP_r}}{\sqrt{\pi}} + \left( t + \frac{z^2 P_r}{2} \right) \text{Erfc} \left( \frac{z\sqrt{P_r}}{2\sqrt{t}} \right),$$

Here  $H(t-1)$  is the Heaviside step function,  $L^{-1}$  indicates the inverse Laplace transform and  $\text{Erfc}(\cdot) = 1 - \text{Erf}(\cdot)$  is the complimentary error function.

Now for finding the concentration profile, putting Eq. (24) into Eq. (19) and using the boundary conditions Eq. (23), we get

$$\bar{\phi}(z, s) = \left( \frac{e^{-z\sqrt{sS_c}}}{s} \right) + a \frac{(1-e^{-s})}{s^2} \left( e^{-z\sqrt{sP_r}} - e^{-z\sqrt{sS_c}} \right) \tag{26}$$

or

$$\phi(z, t) = L^{-1} \left( \frac{e^{-z\sqrt{sS_c}}}{s} \right) + aL^{-1} \left( \frac{e^{-z\sqrt{sP_r}} - e^{-z\sqrt{sS_c}}}{s^2} \right) - aL^{-1} \left\{ e^{-s} \left( \frac{e^{-z\sqrt{sP_r}} - e^{-z\sqrt{sS_c}}}{s^2} \right) \right\}$$

or

$$\phi(z, t) = \text{Erfc} \left( \frac{z\sqrt{S_c}}{2\sqrt{t}} \right) + a\phi_1(z, t) - a\phi_1(z, t-1)H(t-1), \tag{27}$$

here

$$\begin{aligned} \phi_1(z, t) &= L^{-1} \left( \frac{e^{-z\sqrt{sP_r R_a}} - e^{-z\sqrt{sS_c}}}{s^2} \right) \\ &= - \left( t + z^2 \frac{S_c}{2} \right) \text{Erfc} \left( \frac{z\sqrt{S_c}}{2\sqrt{t}} \right) - z\sqrt{\frac{t}{\pi}} \left( e^{-\frac{z^2 P_r}{4t}} \sqrt{P_r} - e^{-\frac{z^2 P_r}{4t}} \sqrt{S_c} \right) + \left( t + \frac{z^2 P_r}{2} \right) \text{Erfc} \left( \frac{z\sqrt{P_r}}{2\sqrt{t}} \right). \end{aligned}$$

By putting Eq. (24) and Eq. (26) into Eq. (20) and using the boundary conditions (21), we get the velocity profile as follows:

$$\bar{V}(z, s) = \frac{e^{-z\sqrt{b+s}}}{s} + \frac{A_3}{s(s-B_2)} \left( e^{-z\sqrt{sS_c}} - e^{-z\sqrt{b+s}} \right) + \frac{1-e^{-s}}{s^2} \frac{(A_1+A_2)}{(s-B_1)} \left( e^{-z\sqrt{P_r}} - e^{-z\sqrt{b+s}} \right) + \frac{1-e^{-s}}{s^2} \frac{aA_3}{(s-B_2)} \left( e^{-z\sqrt{b+s}} - e^{-z\sqrt{sS_c}} \right)$$

or

$$\begin{aligned} V(z, t) &= L^{-1} \left\{ \frac{e^{-z\sqrt{b+s}}}{s} + \frac{A_3}{s(s-B_2)} \left( e^{-z\sqrt{sS_c}} - e^{-z\sqrt{b+s}} \right) \right\} + L^{-1} \left\{ \frac{aA_3}{s^2(s-B_2)} \left( e^{-z\sqrt{b+s}} - e^{-z\sqrt{sS_c}} \right) \right\} \\ &+ L^{-1} \left\{ \frac{(A_1+A_2)}{s^2(s-B_1)} \left( e^{-z\sqrt{P_r}} - e^{-z\sqrt{b+s}} \right) \right\} \\ &- L^{-1} \left[ e^{-s} \left\{ \frac{aA_3}{s^2(s-B_2)} \left( e^{-z\sqrt{b+s}} - e^{-z\sqrt{sS_c}} \right) \right\} \right] - L^{-1} \left[ e^{-s} \left\{ \frac{(A_1+A_2)}{s^2(s-B_1)} \left( e^{-z\sqrt{P_r}} - e^{-z\sqrt{b+s}} \right) \right\} \right] \end{aligned}$$

or

$$V(z, t) = c_1 \{ 2\cosh(k_1 z) + e^{-k_1 z} \text{Erf}(k_1 \sqrt{t} - \eta) - e^{k_1 z} \text{Erf}(k_1 \sqrt{t} + \eta) \} - c_1 e^{k_2^2 t} \{ 2\cosh(k_2 z) \}$$

$$\bar{\theta}(0, s) = \frac{1-e^{-s}}{s^2}, \quad \bar{\theta}(\infty, s) = 0 \tag{22}$$

$$\bar{\phi}(0, s) = \frac{1}{s}, \quad \bar{\phi}(\infty, s) = 0 \tag{23}$$

Where  $\bar{V}(z, s)$ ,  $\bar{\theta}(z, s)$  and  $\bar{\phi}(z, s)$  are the Laplace transform of  $V(z, t)$ ,  $\theta(z, t)$  and  $\phi(z, t)$  respectively.

By using Eq. (22) into Eq. (18), we get,

$$\bar{\theta}(z, s) = \frac{(1-e^{-s})}{s^2} e^{-z\sqrt{sP_r}} \tag{24}$$

Using the property; If  $L^{-1}\{F(s)\} = f(t)$  then  $L^{-1}\{e^{-ms}F(s)\} = f(t-n)H(t-n)$ , the Eq. (24) gives the temperature profile as follows

$$\theta(z, t) = \theta_1(z, t) - \theta_1(z, t-1)H(t-1), \tag{25}$$

$$\begin{aligned}
 & -e^{-k_2z} \operatorname{Erf}(\eta - k_2\sqrt{t}) - e^{k_2z} \operatorname{Erf}(\eta + k_2\sqrt{t}) \} + \frac{1}{2} e^{(k_3^2 - k_1^2)t} \{ 2\cosh(k_3z) - e^{-k_3z} \operatorname{Erf}(\eta - k_3\sqrt{t}) \\
 & - e^{k_3z} \operatorname{Erf}(\eta + k_3\sqrt{t}) \} + c_1 e^{k_5^2 t} \{ 2\cosh(k_4z) + e^{-k_4z} \operatorname{Erf}(k_5\sqrt{t} - k_6\eta) - e^{k_4z} \operatorname{Erf}(k_5\sqrt{t} + k_6\eta) \} \\
 & - 2c_1 \operatorname{Erfc}(k_6\eta) + V_1(z, t) - V_1(z, t-1) H(t-1),
 \end{aligned} \tag{28}$$

$$\begin{aligned}
 \text{here, } V_1(z, t) &= L^{-1} \left\{ \frac{(A_1 + A_2)}{s^2(s - B_1)} \left( e^{-z\sqrt{P_r}} - e^{-z\sqrt{b+s}} \right) \right\} + L^{-1} \left\{ \frac{aA_3}{s^2(s - B_2)} \left( e^{-z\sqrt{b+s}} - e^{-z\sqrt{bS_c}} \right) \right\} \\
 &= -c_2 e^{k_{10}^2 t} \{ 2\cosh(k_7z) - e^{-k_7z} \operatorname{Erf}(\eta - k_7\sqrt{t}) - e^{k_7z} \operatorname{Erf}(\eta + k_7\sqrt{t}) \} + (c_3 t + c_4) \{ 2\cosh(k_1z) \\
 &+ e^{-k_1z} \operatorname{Erf}(k_1\sqrt{t} - \eta) - e^{k_1z} \operatorname{Erf}(k_1\sqrt{t} + \eta) \} + c_5 z \{ 2\sinh(k_1z) + e^{-k_1z} \operatorname{Erf}(k_1\sqrt{t} - \eta) \\
 &- e^{k_1z} \operatorname{Erf}(k_1\sqrt{t} + \eta) \} + c_6 z \sqrt{t} e^{-k_8^2 \eta^2} + c_2 e^{k_{10}^2 t} \{ 2\cosh(k_9z) + e^{-k_9z} \operatorname{Erf}(k_{10}\sqrt{t} - k_8\eta) \\
 &- e^{k_9z} \operatorname{Erf}(k_{10}\sqrt{t} + k_8\eta) \} - (c_7 z^2 + c_8 t + 2c_2) \operatorname{Erfc}(k_8\eta) + c_9 e^{k_5^2 t} \{ 2\cosh(k_2z) - e^{-k_2z} \operatorname{Erf}(\eta - k_2\sqrt{t}) \\
 &- e^{k_2z} \operatorname{Erf}(\eta + k_2\sqrt{t}) \} - c_{10} z \sqrt{t} e^{-k_6^2 \eta^2} - c_9 e^{k_5^2 t} \{ 2\cosh(k_4z) + e^{-k_4z} \operatorname{Erf}(k_5\sqrt{t} - k_6\eta) \\
 &+ (c_{12} z^2 + c_{11} t + 2c_9) \operatorname{Erfc}(k_6\eta) \}.
 \end{aligned}$$

2.1. Solution for an isothermal plate:

For the case of an isothermal plate, the solutions for concentration, temperature and velocity profiles are obtained as flows:

$$\theta_{iso}(z, t) = \operatorname{Erfc}(k_8\eta) \tag{29}$$

$$\phi_{iso}(z, t) = (1-a) \operatorname{Erfc}(k_6\eta) + a \operatorname{Erfc}(k_8\eta) \tag{30}$$

$$\begin{aligned}
 V_{iso}(z, t) &= (c_1 + c_3) \{ 2\cosh(k_1z) + e^{-k_1z} \operatorname{Erf}(k_1\sqrt{t} - \eta) - e^{k_1z} \operatorname{Erf}(k_1\sqrt{t} + \eta) \} \\
 &- \frac{c_8}{2} e^{k_{10}^2 t} \{ 2\cosh(k_7z) - e^{-k_7z} \operatorname{Erf}(\eta - k_7\sqrt{t}) - e^{k_7z} \operatorname{Erf}(\eta + k_7\sqrt{t}) \} \\
 &- (1-a)c_1 e^{k_5^2 t} \{ 2\cosh(k_2z) - e^{-k_2z} \operatorname{Erf}(\eta - k_2\sqrt{t}) - e^{k_2z} \operatorname{Erf}(\eta + k_2\sqrt{t}) \} \\
 &+ \frac{1}{2} e^{(k_3^2 - k_1^2)t} \{ 2\cosh(k_3z) - e^{-k_3z} \operatorname{Erf}(\eta - k_3\sqrt{t}) - e^{k_3z} \operatorname{Erf}(\eta + k_3\sqrt{t}) \} \\
 &+ \frac{c_8}{2} e^{k_{10}^2 t} \{ 2\cosh(k_9z) + e^{-k_9z} \operatorname{Erf}(k_{10}\sqrt{t} - k_8\eta) - e^{k_9z} \operatorname{Erf}(k_{10}\sqrt{t} + k_8\eta) \} \\
 &- c_8 \operatorname{Erfc}(k_8\eta) - 2c_1(1-a) \operatorname{Erfc}(k_6\eta) + (1-a)c_1 e^{k_5^2 t} \{ 2\cosh(k_4z) \\
 &+ e^{-k_4z} \operatorname{Erf}(k_5\sqrt{t} - k_6\eta) - e^{k_4z} \operatorname{Erf}(k_5\sqrt{t} + k_6\eta) \},
 \end{aligned} \tag{31}$$

here

$$\begin{aligned}
 b &= M + 2i\Omega + \frac{1}{K}, \quad a = \frac{P_r S_r S_c}{S_c - P_r}, \quad A_1 = \frac{G_r}{1 - P_r}, \quad A_2 = \frac{aG_m}{1 - P_r}, \quad A_3 = \frac{G_m}{1 - S_c}, \quad B_1 = \frac{b}{P_r - 1}, \quad B_2 = \frac{b}{S_c - 1}, \quad c_1 = \frac{A_3}{2B_2}, \\
 c_2 &= \frac{A_1 + A_2}{2B_1^2}, \quad c_3 = \frac{A_1 + A_2}{2B_1} - \frac{aA_3}{2B_2}, \quad c_4 = \frac{A_1 + A_2}{2B_1^2} - \frac{aA_3}{2B_2^2}, \quad c_5 = \frac{A_1 + A_2}{4B_1\sqrt{b}} - \frac{aA_3}{4B_2\sqrt{b}}, \quad c_6 = \frac{\sqrt{P_r}(A_1 + A_2)}{B_1\sqrt{\pi}}, \\
 c_7 &= \frac{P_r(A_1 + A_2)}{2B_1}, \quad c_8 = \frac{A_1 + A_2}{B_1}, \quad c_9 = \frac{aA_3}{2B_2^2}, \quad c_{10} = \frac{aA_3}{B_2} \sqrt{\frac{S_c}{\pi}}, \quad c_{11} = \frac{aA_3}{B_2}, \quad c_{12} = \frac{aA_3 S_c}{2B_2}, \quad k_1 = \sqrt{b}, \quad k_2 = \sqrt{b + B_2}, \\
 k_3 &= \sqrt{b}, \quad k_4 = \sqrt{B_2 S_c}, \quad k_5 = \sqrt{B_2}, \quad k_6 = \sqrt{S_c}, \quad k_7 = \sqrt{b + B_1}, \quad k_8 = \sqrt{P_r}, \quad k_9 = \sqrt{B_1 P_r}, \quad k_{10} = \sqrt{B_1}, \quad \eta = \frac{z}{2\sqrt{t}}.
 \end{aligned}$$

2.2. Skin Friction coefficient, Sherwood Number and Nusselt Number:

The shear stress is given by

$$-\mu \frac{\partial V}{\partial z} = -\mu \frac{\partial(u + iv)}{\partial z} = -\mu \frac{\partial u}{\partial z} - i\mu \frac{\partial v}{\partial z}$$

If  $\tau_x$  and  $\tau_y$  be the components of shear stress in the primary and secondary directions respectively, then

$$\tau_x = -\mu \frac{\partial u}{\partial z} \text{ and } \tau_y = -\mu \frac{\partial v}{\partial z}.$$

By using non-dimensional parameters given in Eq. (6), the dimensionless stresses are

$$\tau_1(z', t') = \frac{\tau_x}{\tau_o} = -\frac{\partial u'}{\partial z'} \text{ and } \tau_2(z', t') = \frac{\tau_y}{\tau_o} = -\frac{\partial v'}{\partial z'} \text{ where } \tau_o = \rho u_o^2.$$

Consider the complex notation i.e.  $\tau(z', t') = \tau_1(z', t') + i\tau_2(z', t')$  and after omitting the prime ('), the non-dimensional shear stress changes to:

$$\tau(z, t) = \tau_1(z, t) + i\tau_2(z, t) = -\frac{\partial V(z, t)}{\partial z}$$

Therefore, the non-dimensional coefficients of skin friction at the plate in complex form is given as

$$\begin{aligned} [S_f(t)]_{ramped} &= \tau(0, t) \\ &= \frac{1}{\sqrt{\pi t}} \left( 2c_1 e^{-k_1^2 t} + e^{-k_2^2 t} - 2c_1 e^{(k_5^2 - k_2^2)t} \right) + 2c_1 k_1 \operatorname{erf}(k_1 \sqrt{t}) - 2c_1 k_2 e^{k_5^2 t} \operatorname{erf}(k_2 \sqrt{t}) \\ &+ k_3 e^{(k_5^2 - k_1^2)t} \operatorname{erf}(k_3 \sqrt{t}) + 2c_1 k_4 e^{k_5^2 t} \operatorname{erf}(k_5 \sqrt{t}) + S_1(t) - S_1(t-1)H(t-1), \end{aligned} \quad (32)$$

Where

$$\begin{aligned} S_1(t) &= \frac{1}{\sqrt{\pi t}} \{ 2(c_3 t + c_4) e^{-k_1^2 t} + 2c_9 e^{(k_5^2 - k_2^2)t} + (k_6 c_{11} - k_8 c_8) t - 2c_2 e^{(k_{10}^2 - k_7^2)t} \} + (c_{10} - c_6) \sqrt{t} \\ &+ \{ 2k_1 (c_3 t + c_4) + 2c_3 \} \operatorname{erf}(k_1 \sqrt{t}) + 2c_9 k_2 e^{k_5^2 t} \operatorname{erf}(k_2 \sqrt{t}) \\ &- 2c_9 k_4 e^{k_5^2 t} \operatorname{erf}(k_5 \sqrt{t}) - 2c_2 k_7 e^{k_{10}^2 t} \operatorname{erf}(k_7 \sqrt{t}) + 2c_2 k_9 e^{k_{10}^2 t} \operatorname{erf}(k_{10} \sqrt{t}). \end{aligned}$$

$$\begin{aligned} [S_f(t)]_{iso} &= \tau(0, t) = \frac{1}{\sqrt{\pi t}} \{ (2c_1 + 2c_3 + 1) e^{-k_1^2 t} - 2c_1 (1-a) e^{(k_5^2 - k_2^2)t} - c_8 e^{(k_{10}^2 - k_7^2)t} \} + 2k_1 (c_1 + c_3) \operatorname{erf}(k_1 \sqrt{t}) \\ &- 2c_1 k_2 (1-a) e^{k_5^2 t} \operatorname{erf}(k_2 \sqrt{t}) + k_3 e^{(k_5^2 - k_1^2)t} \operatorname{erf}(k_3 \sqrt{t}) + 2c_1 k_4 (1-a) e^{k_5^2 t} \operatorname{erf}(k_5 \sqrt{t}) \\ &- c_8 k_7 e^{k_{10}^2 t} \operatorname{erf}(k_7 \sqrt{t}) + c_8 k_9 e^{k_{10}^2 t} \operatorname{erf}(k_{10} \sqrt{t}) \end{aligned} \quad (33)$$

Hence, the non-dimensional coefficients of skin friction in the primary and secondary directions respectively can be found as:

$$S_{f_x} = \operatorname{Re}(S_f) \text{ and } S_{f_y} = \operatorname{Im}(S_f)$$

Again, by using Eq. (6), non-dimensional Sherwood and Nusselt number are obtained as follows:

The rate of change of concentration at the plate i.e. Sherwood number for both the cases are:

$$[Sh]_{ramped} = -\left( \frac{\partial \phi}{\partial z} \right)_{z=0} = \sqrt{\frac{S_c}{\pi t}} + \frac{2a}{\sqrt{\pi}} (\sqrt{P_r} - \sqrt{S_c}) \{ \sqrt{t} - \sqrt{t-1} H(t-1) \} \quad (34)$$

$$[Sh]_{iso} = -\left( \frac{\partial \phi}{\partial z} \right)_{z=0} = \frac{1}{\sqrt{\pi t}} \{ a \sqrt{P_r} + (1-a) \sqrt{S_c} \} \quad (35)$$

The rate of change of temperature at the plate i.e. Nusselt number for both the cases are:

$$[N_u]_{ramped} = -\left( \frac{\partial \theta}{\partial z} \right)_{z=0} = 2 \sqrt{\frac{P_r t}{\pi}} - 2 \sqrt{\frac{P_r (t-1)}{\pi}} H(t-1) \quad (36)$$

$$[N_u]_{iso} = -\left( \frac{\partial \theta}{\partial z} \right)_{z=0} = \sqrt{\frac{P_r}{\pi t}} \quad (37)$$

3. Figures

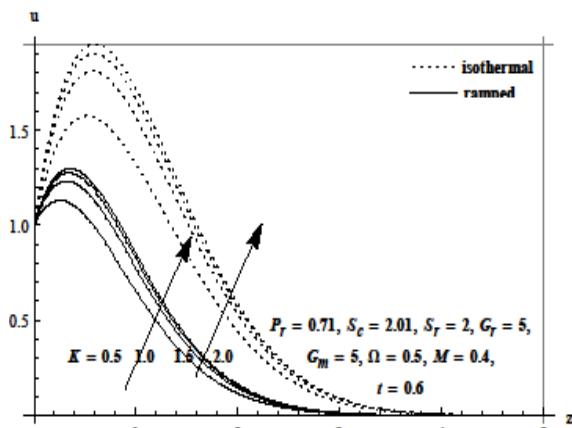


Figure 2. Primary Velocity profile for  $K$

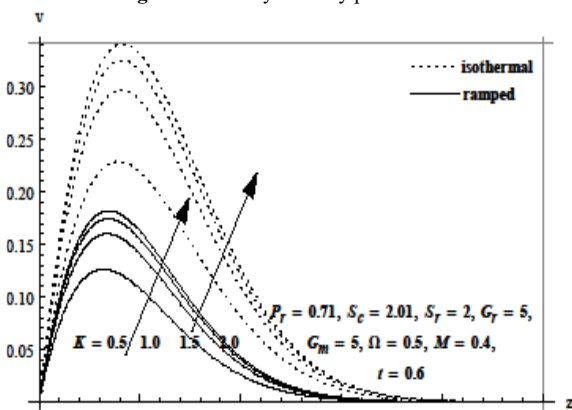


Figure 3. Secondary Velocity profile for  $K$

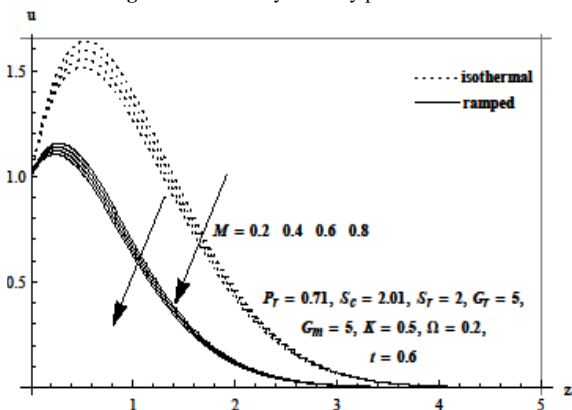


Figure 4. Primary Velocity profile for  $M$

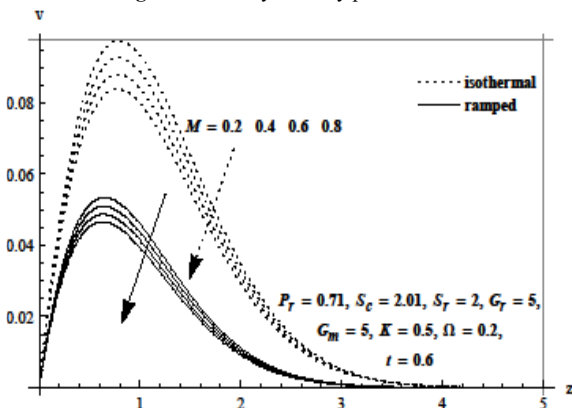


Figure 5. Secondary Velocity profile for  $M$

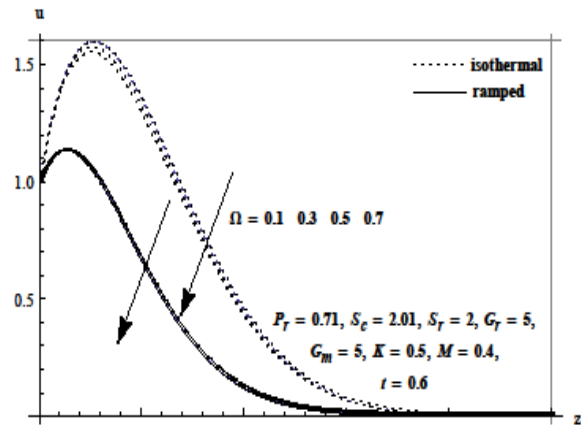


Figure 6. Primary Velocity profile for  $\Omega$

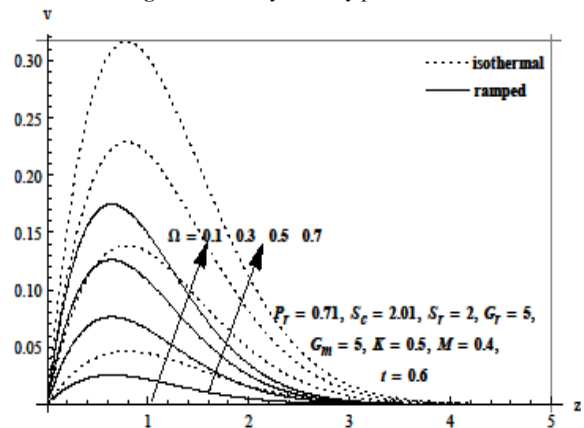


Figure 7. Secondary Velocity profile for  $\Omega$

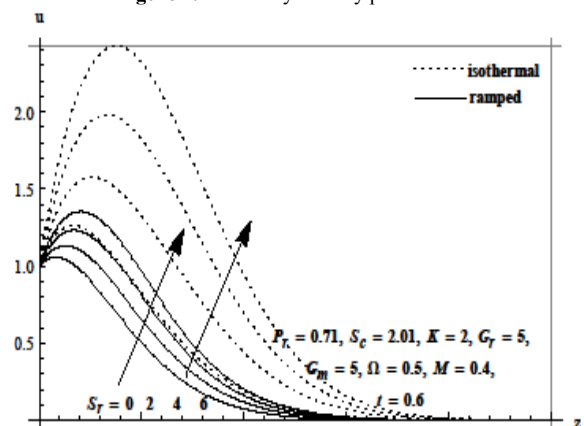


Figure 8. Primary Velocity profile for  $S_r$

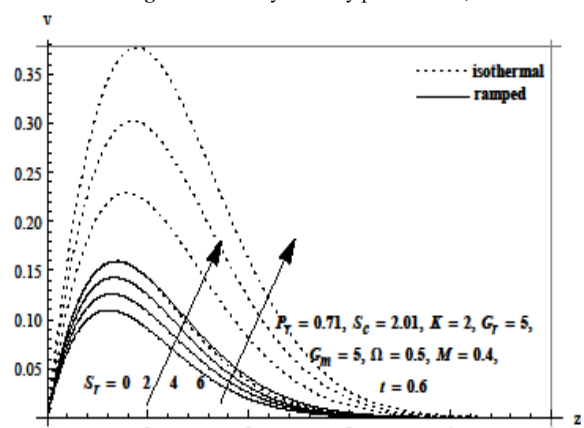


Figure 9. Secondary Velocity profile for  $S_r$

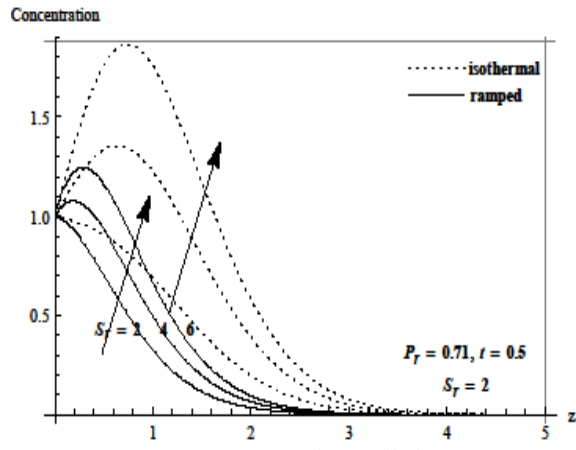


Figure 10. Concentration profile for  $S_r$

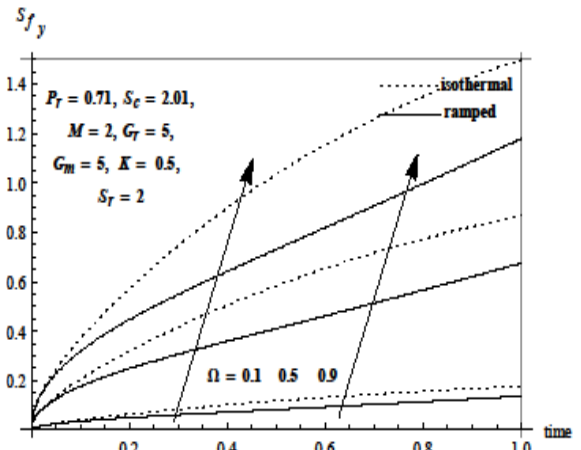


Figure 14. Secondary Skin Friction profile for  $\Omega$

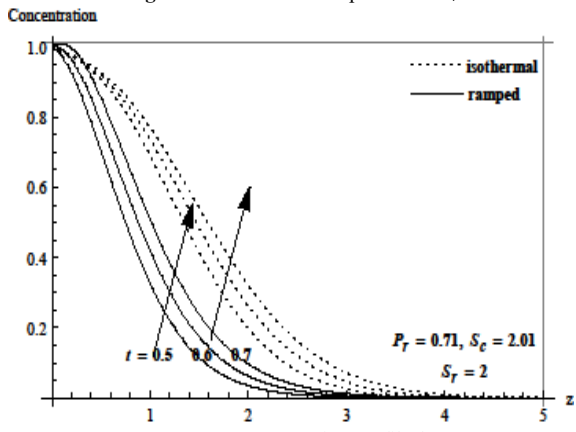


Figure 11. Concentration profile for  $t$

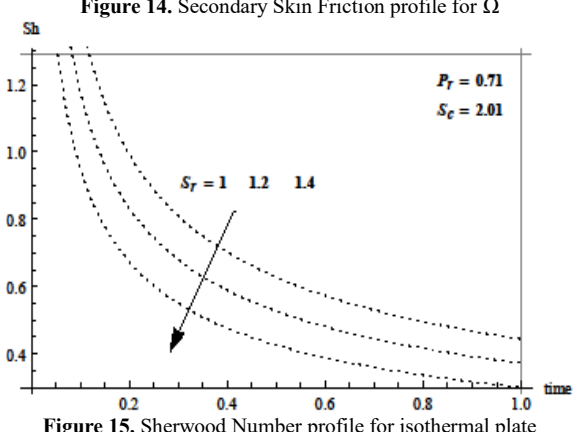


Figure 15. Sherwood Number profile for isothermal plate temperature with  $S_r$

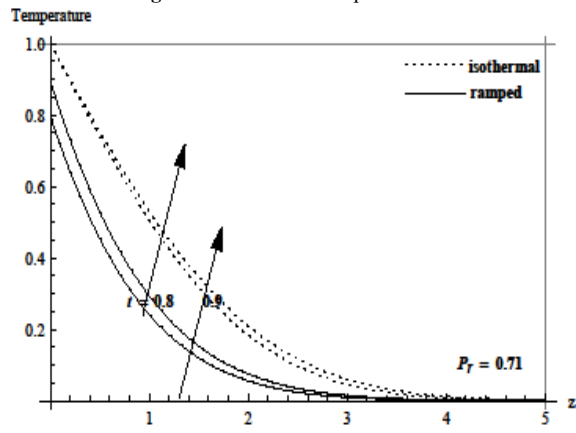


Figure 12. Temperature profile for  $t$

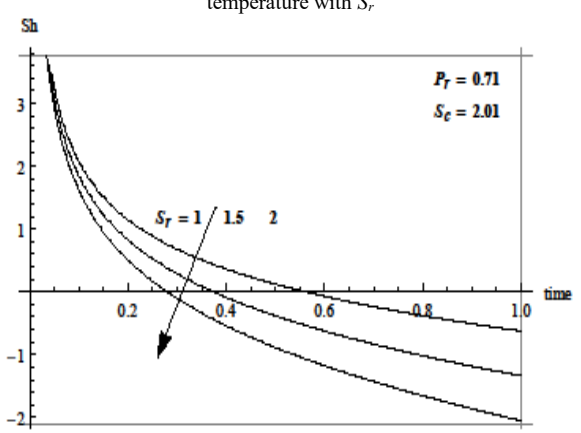


Figure 16. Sherwood Number profile for ramped plate temperature with  $S_r$

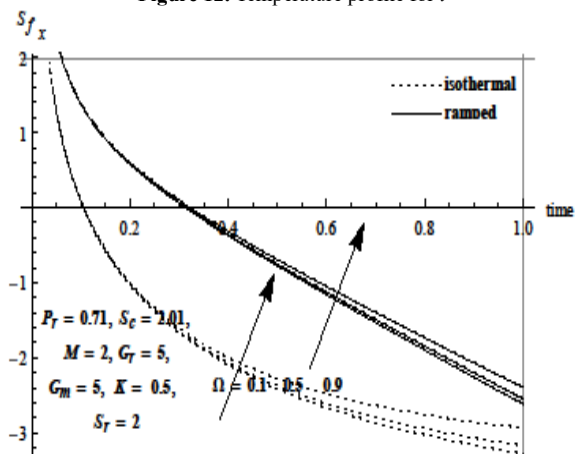


Figure 13. Primary Skin Friction for  $\Omega$

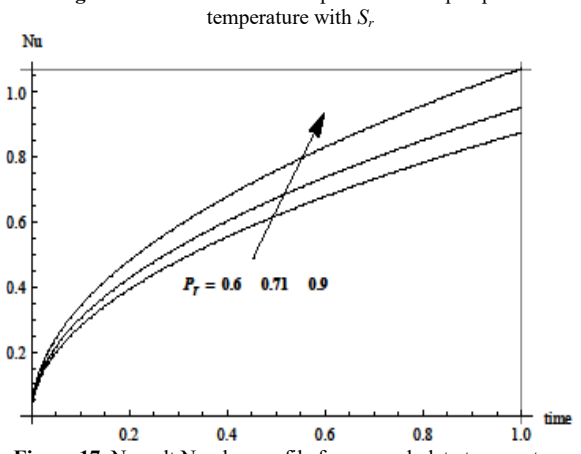


Figure 17. Nusselt Number profile for ramped plate temperature with time



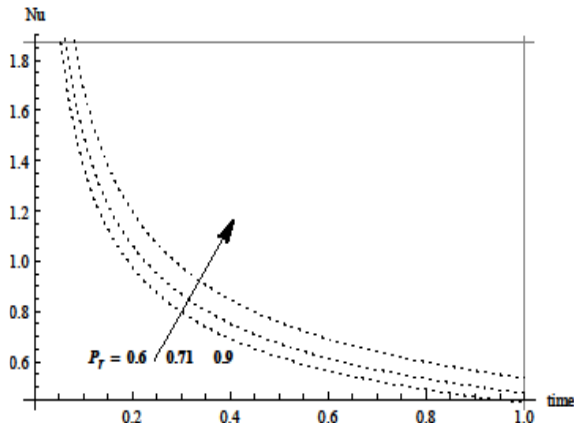


Figure 18. Nusselt Number profile for isothermal plate temperature with time

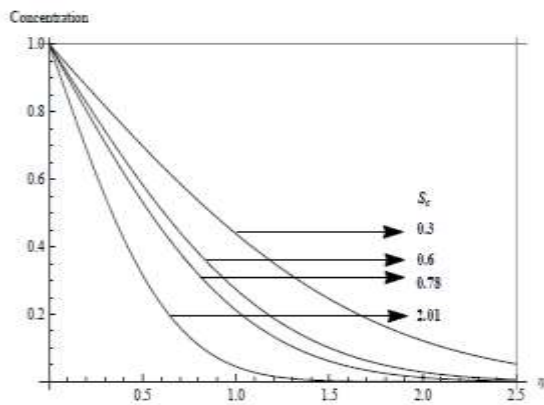


Figure 19. Concentration profile for  $S_c$

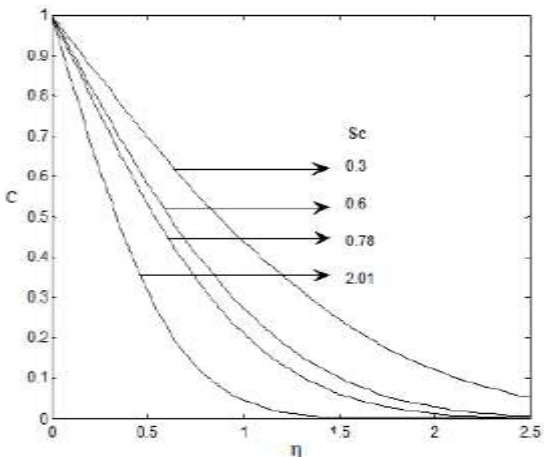


Figure 20. Scanned graph of Concentration profile when  $t = 0.2$  at different values of  $S_c$  drawn by Muthucumaraswamy and Prema[4]

4. Results and Discussion

In order to show the physical changes of some parameters of interest on the obtained solution, the analytical results for velocity, concentration, temperature, Skin friction, Sherwood number and Nusselt number are shown graphically in Figs.2-20. The Figs.2-9 shows the variation in the magnitude of primary and secondary fluid velocities in the boundary layer region versus boundary layer coordinate for various values of permeability parameter  $K$ , Soret number  $S_r$ , Magnetic parameter  $M$  and rotation parameter  $\Omega$  taking  $G_r = 5$ ,  $G_m = 5$ ,  $t = 0.6$ ,  $P_r =$

0.71 and  $S_c = 2.01$ . For both ramped and isothermal temperature plates; it is observed that, primary fluid velocity  $u$  (velocity along plate) and secondary fluid velocity  $v$  (velocity transverse to plate) acquire a different maximum value in the vicinity of the plate and then decrease gradually to approach free stream value. The effect of porosity of the medium on the velocity field can be shown in Fig. 2 and 3. It is observed that both the components of the velocity increase with the increase in the permeability parameter  $K$ ; it is in good agreement with the fact that a porous medium with large value of permeability parameter will support the movement of the fluid through it. Also, the Fig.4 and 5 reveals that an increase in the magnetic parameter  $M$  can decrease the primary and increase the secondary fluid velocities. Physically it is due to the fact that if we apply a transverse magnetic field towards the flow, it will offer a Lorentz force which acts in the transverse direction and hence resists the primary flow. Furthermore, the effect of rotation parameter can be seen from Fig.6 and 7. It is noticed that for both isothermal and ramped temperature plates, the primary fluid velocity decreases and the secondary fluid velocity increases with increase in the rotation parameter. Hence rotation has tendency to accelerate the secondary flow and retards the flow in the primary direction. Physically it is in good agreement with the Coriolis force which has a tendency to enhance the secondary flow and suppress the primary flow. It is also evident from Fig.8 and 9 that the primary as well as secondary fluid velocity increases with the increase in  $S_r$ . Whereas for both isothermal and ramped temperature plates we noticed in the Fig.10 and 11 that concentration within the boundary layer increases with increase in  $S_r$  or  $t$ . Also, temperature of the system increases with time (Fig.12). For both ramped and isothermal temperature plates, the effect of different governing parameters on Skin-friction, Sherwood number  $Sh$  and Nusselt number  $N_u$  are shown in Figs. 13-18. From Fig.13 and 14, it is evident that, the primary skin friction i.e.  $S_{fx}$  and magnitude of secondary skin friction i.e.  $S_{fy}$  increase with increase in  $\Omega$ . The rates of mass transfer is measured by Sherwood number  $Sh$  and Fig. 15 and 16 reveals variation in  $Sh$  with the soret number, for both isothermal and ramped temperature plates; it is found that  $S_h$  decreases with the increase in  $S_r$ . Nusselt number  $N_u$  measure the heat transfer rate at the plate and Fig.17 and 18 depicts the changes in the values of Nusselt number with Prandtl number. For both isothermal and ramped temperature plates, Nusselt number increases on increasing  $P_r$ . Further, for isothermal plate,  $N_u$  decreases with the increase in time. On the other hand, for ramped temperature, it increases on increasing  $t$ .

5. Conclusion

For both isothermal and ramped temperature plates; it is found that primary fluid velocity and secondary fluid velocity attain a different maximum value in the vicinity of the plate and then decrease gradually. Other conclusions are as follows:

- Larger value of magnetic field and rotation decreases the primary fluid velocity, and increases the magnitude of secondary fluid velocity.

- The amplitude of temperature, velocity and concentration fields for isothermal plate are always larger than ramped plate temperature.
- The magnitude of dimensionless velocities increases with an increase in the permeability of porous medium.
- The increase in either Soret number or time causes the decrease in Sherwood number.

Also, the model under consideration can be expanded into the studies of the flow past spheres, cylinders, cones, and wedges etc., according to the required applications.

### Comparison of Result

To check the validity of our result, we have compared one of our results with R. Muthucumaraswamy and K. M. A. Prema[3]. They considered the Hall effects on flow past an exponentially accelerated infinite isothermal vertical plate with mass diffusion. In absence of Soret effect i.e. taking  $S_r = 0$  expression of concentration field of the present problem is  $\phi_{iso}(z, t) = \text{Erfc}(k_0 \eta)$ . Fig.19 and Fig. 20 show the concentration profile for different values of  $S_c$  obtained by present author and Muthucumaraswamy & Prema[3] respectively. Schmidt number  $S_c$  is a dimensionless number defined as the ratio of momentum diffusivity (viscosity) and mass diffusivity of the fluid. It physically relates the relative thickness of the hydrodynamic layer and mass-transfer boundary layer. For Ethyl Benzene the value of Schmidt number  $S_c$  is 2.01. Both figures uniquely express the fact that concentration in the system decreases for increasing values of Schmidt number. Hence, an excellent agreement of results between present author and Muthucumaraswamy & Prema[3] is observed.

### References

- [1] Jaimala, Vikrant, K. Vivek, "Thermal convection in a Couple-Stress fluid in the presence of horizontal magnetic field with Hall currents". *Application and Applied Mathematics*, Vol. 8, No. 1, 2013, 161-117.
- [2] T. Vijaya Laxmi, Bandari Shankar, "Radiative boundary layer flow and heat transfer of nanofluid over a nonlinear stretching sheet with slip conditions and suction". *Jordan Journal of Mechanical and Industrial Engineering*, Vol.10, No. 4, 2016, 285 - 297.
- [3] R. Muthucumaraswamy, K. M. A. Prema, "Hall effects on flow past an exponentially accelerated infinite isothermal vertical plate with mass diffusion". *J. of App. Fluid Mech.*, Vol.9, No. 2, 2016, 889-897.
- [4] Branover, H. *Magnetohydrodynamic Flow in Ducts*. John Wiley and Sons, New York; 1978.
- [5] S. Ravi Kumar, "The effect of the couple stress fluid flow on MHD peristaltic motion with uniform porous medium in the presence of slip effect". *Jordan Journal of Mechanical and Industrial Engineering*, Vol.9, No. 4, 2015, 269 - 278.
- [6] E. Osalusi, P. Sibanda, "On variable laminar convection flow properties due to a porous rotating disk in a magnetic field". *Romania Journal of Physics*, Vol.51, No. 9-10, 2006, 937-950.
- [7] A. M. Jawarneh, Mohamad Al-Widyan, Zain Al-Mashhadani, "Experimental study on heat transfer augmentation in a double pipe heat exchanger utilizing jet vortex flow". *Heat Transfer*, Vol. 52, No. 1, 2023, 317-332.
- [8] Cowling, T.G. *Magnetohydrodynamics*. Interscience, New York; 1957.
- [9] Khilap Singh, Manoj Kumar, "The effect of chemical reaction and double stratification on MHD free convection in a micropolar fluid with heat generation and ohmic heating". *Jordan Journal of Mechanical and Industrial Engineering*, Vol.9, No. 4, 2015, 279 - 288.
- [10] Bala Siddulu Malga, Naikoti Kishan, V.V Reddy, K. Govardhan, "Finite element analysis of fully developed free convection flow heat and mass transfer of a MHD / Micropolar Fluid over a vertical channel". *Jordan Journal of Mechanical and Industrial Engineering*, Vol.8, No. 4, 2014, 219 - 232.
- [11] Y.J. Kim, "Heat and mass transfer in MHD Micropolar flow over a vertical moving porous plate in a porous medium". *Transport in Porous Media*, Vol. 56, No. 1, 2004, 17-37.
- [12] Mohammad A. Hamdan, Anwar H. Al-Assaf, Mohammad A. Al-Nimr, "Effect of transverse steady magnetic field on MHD flow under free convection conditions in vertical microchannels". *Jordan Journal of Mechanical and Industrial Engineering*, Vol.12, No. 2, 2018, 131 - 139.
- [13] Owen J. M., Rogers R. H. *Flow and heat transfer in rotating disc systems*. Vol.I, Rotor - Stator Systems, John Wiley Sons, New York; 1989.
- [14] Greenspan, H. P. *The Theory of Rotating Fluids*. Cambridge University Press. London; 1968.
- [15] A.M. Jawarneh, "Heat transfer enhancement in a narrow concentric annulus in decaying swirl flow". *Heat Transfer Research*, Vol. 42, No. 3, 2011, 199-216.
- [16] Platten, J.K., "The Soret effect: A review of recent experimental results". *Journal of applied mechanics*, Vol. 73, 2006, 5-15.
- [17] R. Bhargava, R. Sharma, O. A. Beg, "Oscillatory chemically-reacting MHD free convection heat and mass transfer in a porous medium with Soret and Dufour effects: finite element modeling". *Int. J. Applied Mathematics and Mechanics*, Vol. 5, No. 6, 2009, 15-37.
- [18] A. Postelnicu, "Influence of a magnetic field on heat and mass transfer by natural convection from vertical surfaces in porous media considering Soret and Dufour effects". *Int. J. Heat & Mass Transfer*, Vol. 47, 2004, 1467-1472.
- [19] A. Postelnicu, "Influence of chemical reaction on heat and mass transfer by natural convection from vertical surfaces in porous media considering Soret and Dufour effects". *Heat Mass Transfer*, Vol. 43, 2007, 595-602.
- [20] O.A. Beg, T. A. Beg, A.Y. Bakier, V.R. Prasad, "Chemically-reacting mixed convective heat and mass transfer along inclined and vertical plates with Soret and Dufour effects: Numerical solutions". *Int. J. Applied Mathematics and Mechanics*, Vol. 5, No. 2, 2009, 39-57.
- [21] M.S. Alam, M.M. Rahman, "Dufour and Soret effects on mixed convection flow past a vertical porous flat plate with variable suction", *Nonlinear Analysis: Modelling and Control*, Vol.11, No. 1, 2006, 3-12.
- [22] A.A. Ibrahim, "Analytic solution of heat and mass transfer over a permeable stretching plate affected by chemical reaction, internal heating, Dufour-Soret effect and Hall effect". *Thermal science*, Vol. 13, No. 2, 2009, 183-197.
- [23] Rajput, U.S., M. Shareef, "Analysis of chemical reaction and thermophoresis on MHD flow near the accelerated vertical plate in a rotating system with variable temperature". *Jour. Comp. & App. Res. in Mech. Eng.*, Vol. 10, No. 2, 2021, 449-460.
- [24] M. Anil Kumar, Y. Dharmendar Reddy, B. Shankar Goud, V. Srinivasa Rao, "Effects of Soret, Dufour, Hall current and rotation on MHD natural convective heat and mass transfer flow past an accelerated vertical plate through a porous medium". *International Journal of Thermofluids*, Vol. 9, 2021, 100061.

- [25] M. A. Imran, D. Vieru, I. A. Mirza, "The influence of ekman number on flows over an oscillating isothermal vertical plate in a rotating frame". *Journal of Applied Fluid Mechanics*, Vol. 8, No. 4, 2015, 781-791.
- [26] G.S. Seth, R. Nandkeolyar, M. S. Ansari, "Effects of thermal radiation and rotation on unsteady hydromagnetic free convection flow past an impulsively moving vertical plate with ramped temperature in a porous medium". *Journal of Applied Fluid Mechanics*, Vol. 6, No. 1, 2013, 27-38.
- [27] Ziya Uddin, Manoj Kumari, "MHD Heat and Mass transfer free convection flow near the lower stagnation point of an isothermal cylinder imbedded in Porous Domain with the presence of Radiation". *Journal of Applied Fluid Mechanics*, Vol. 5, No. 5, 2011, 419-423.
- [28] Ziya Uddin, Manoj Kumar, "MHD Heat and Mass transfer free convection flow near the lower stagnation point of an isothermal cylinder imbedded in Porous Domain with the presence of Radiation". *Journal of Applied Fluid Mechanics*, Vol. 5, No. 2, 2011, 133-138.